Pergamon

0301-9322(95)00023-2

Int. J. Multiphase Flow Vol. 21, No. 5, pp. 941–947, 1995

0301-9322/95 $9.50 + 0.00

BRIEF COMMUNICATION

HEAD-ON INTERACTION OF WEAK PLANAR SHOCK WAVES WITH FLEXIBLE POROUS MATERIALS—ANALYTICAL MODEL

H. LI and G. BEN-DOR

Pearlstone Center for Aeronautical Engineering Studies, Department of Mechanical Engineering, Ben-Gurion University of the Negev, Beer Sheva, Israel

(Received 3 April 1994; in revised form 14 March 1995)

INTRODUCTION

In a recent study, Skews (1991) reported on a series of shock tube experiments in which the interaction of weak planar shock waves with low density foams was investigated. Baer (1992) presented an analytical model, based on the continuum mixture theory, for describing the shock–foam interaction phenomena. His numerical simulations were found to agree quite well with Skews' (1991) experiments. Olim *et al.* (1994) also recently simulated the same experiments but used a completely different approach. In fact, they adopted a pseudo-gas model which was originally proposed by Rudinger (1965). In this approach the two-phase medium, i.e. the gaseous phase and the skeleton of which the foam is made, is treated as a homogeneous pseudo-gas. Consequently, the problem is reduced to the refraction of a shock wave at a gaseous interface.

The pseudo-gas approach was also adopted in the course of the present study. However, since immediately behind shock waves $T_G > T_p$ our model, as will be shown subsequently, is different. In addition, unlike Baer (1992) and Olim *et al.* (1994) whose investigations were numerical, we present an analytical investigation. Our model is limited to analytically predicting the flow field in the vicinity of the gas–foam interface immediately after the front edge of the foam was struck head-on by the planar shock wave. This limitation arises from the fact that, unlike Gelfand *et al.* (1983) and Gvozdeva *et al.* (1985) who assumed that the wave transmitted into the foam is a shock wave and remains a shock wave while propagating inside the foam, our model accounts for the fact that the transmitted shock wave changes into a dispersed wave.

PRESENT STUDY

Based on Igra & Ben-Dor (1988), the one-dimensional conservation equations of the flow of a dust–gas suspension are:

$$\frac{\partial U}{\partial t} + \frac{\partial F}{\partial x} = G \qquad [1a]$$

where U, F and G are, respectively

$$U = \begin{bmatrix} \rho_G \\ \rho_p \\ \rho_G u_G \\ \rho_p u_p \\ \rho_G\left(e_G + \frac{u_G^2}{2}\right) \\ \rho_p\left(e_p + \frac{u_p^2}{2}\right) \end{bmatrix}, \quad F = \begin{bmatrix} \rho_G u_G \\ \rho_p u_p \\ \rho_G u_G^2 + p \\ \rho_p u_p^2 \\ \rho_G u_G\left(h_G + \frac{u_G^2}{2}\right) \\ \rho_p u_p\left(h_p + \frac{u_p^2}{2}\right) \end{bmatrix} \quad \text{and} \quad G = \begin{bmatrix} 0 \\ 0 \\ -F_D \\ F_D \\ -Q_{HT} - F_D u_p \\ Q_{HT} + F_D u_p \end{bmatrix} \qquad [1b]$$

Here ρ, u, e, p and h are density, velocity, internal energy, pressure and enthalpy, respectively. F_D and Q_{HT} are the drag force and the heat transfer per unit volume, respectively. The subscripts "p" and "G" refer to the dust (solid particles) and gaseous phases, respectively.

If the discussion is limited to the vicinity of the front edge of the foam and if it is assumed that the incident shock induced flow does not penetrate the foam, then

$$\bar{u} = u_G = u_p \tag{2}$$

The use of [2] is further justified by Skews *et al.*'s (1993) finding that "the foam face moves at approximately the gas velocity ahead of the foam".

The two-phase suspension can be transformed into a single-phase medium by means of the following definitions:

$$\bar{\rho} = \rho_G + \rho_p, \quad \bar{p} = p, \quad \bar{\rho}\bar{e} = \rho_G e_G + \rho_p e_p, \quad \bar{\rho}\bar{h} = \rho_G h_G + \rho_p h_p,$$
$$\bar{e} = \bar{C}_v \bar{T} \quad \text{and} \quad \bar{h} = \bar{C}_p \bar{T} \tag{3}$$

where

$$\bar{C}_v = \frac{\rho_G C_v + \rho_p C_m}{\rho_G + \rho_p} \quad \text{and} \quad \bar{C}_p = \frac{\rho_G C_p + \rho_p C_m}{\rho_G + \rho_p} \tag{4}$$

Inserting the new single-phase parameters, as defined by [3] and [4] into [1] results in:

$$\bar{U} = \begin{bmatrix} \bar{\rho} \\ \bar{\rho}\bar{u} \\ \bar{\rho}\left(\bar{e} + \frac{\bar{u}^2}{2}\right) \end{bmatrix}, \quad \bar{F} = \begin{bmatrix} \bar{\rho}\bar{u} \\ \bar{\rho}\bar{u}^2 + \bar{p} \\ \bar{\rho}\bar{u}\left(\bar{h} + \frac{\bar{u}^2}{2}\right) \end{bmatrix} \quad \text{and} \quad \bar{G} = \begin{bmatrix} 0 \\ 0 \\ 0 \end{bmatrix} \tag{5}$$

Equation [5] is identical in its form to the conservation equations of a pure gas. However, since these equations originate from those of a two-phase mixture, they will be referred to, in the following, as the conservation equations of a "pseudo-gas". Rearranging [3] results in:

$$\bar{T} = \frac{\rho_G C_v T_G + \rho_p C_m T_p}{\rho_G C_v + \rho_p C_m} \tag{6a}$$

Note that unlike Rudinger (1965), Gelfand *et al.* (1983) and Gvozdeva *et al.* (1985), in the present case the assumption $T_G = T_p$ is not required and hence not used. This equation can be rewritten with the addition of the loading ratio, $\eta = \rho_p/(\rho_p + \rho_G)$, to read:

$$\bar{T} = \frac{(1-\eta)C_v T_G + \eta C_m T_p}{(1-\eta)C_v + \eta C_m} \tag{6b}$$

Similarly, [4] can be rewritten as:

$$\bar{C}_v = (1-\eta)C_v + \eta C_m \quad \text{and} \quad \bar{C}_p = (1-\eta)C_p + \eta C_m \tag{7}$$

Using these two relations the specific heat capacities ratio, $\bar{\gamma}$, is

$$\bar{\gamma} = \frac{\bar{C}_p}{\bar{C}_v} = \frac{(1-\eta)C_p + \eta C_m}{(1-\eta)C_v + \eta C_m} = \frac{\gamma(1-\eta+\eta\delta)}{(1-\eta+\gamma\eta\delta)} \tag{8}$$

where $\delta = C_m/C_p$. Equations [7] can be used to also define the pseudo-gas constant $\bar{R}$:

$$\bar{R} = \bar{C}_p - \bar{C}_v = (1-\eta)(C_p - C_v) = (1-\eta)R \tag{9}$$

where R is the specific gas constant of the gaseous phase of the suspension. Thus the speed of sound and flow Mach number of the pseudo-gas are

$$(\bar{a})^2 = \bar{\gamma}\bar{R}\bar{T} \quad \text{and} \quad \bar{M} = \bar{u}/\bar{a} \tag{10}$$

The finally obtained set of equations, which could be written follows

$$\frac{\partial \bar{U}}{\partial t} + \frac{\partial \bar{F}}{\partial x} = 0 \qquad [11]$$

is, in fact, identical to the conservation equations of a pure gas. Consequently, analytical solutions which exist in phenomena involving pure gases (e.g. the well-known Rankine–Hugoniot relations across planar shock waves) can readily be used in identical phenomena using pseudo gases with the appropriate transformation of the gas properties.

The analytical model

Consider figure 1(a) in which a constant velocity planar shock wave is seen to propagate from left to right towards a flexible porous material. The flow states ahead and behind the incident shock waves are (0) and (1), respectively. The flow state inside the porous medium is (2). The front edge of the porous material is marked by P. The incident shock wave Mach number is M_i. The wave pattern which is obtained following the head-on reflection of the incident shock wave from the front edge of the flexible porous material is shown in figure 1(b). It consists of a reflected shock wave, having a Mach number M_r, and a transmitted shock wave, having a Mach number M_t. The reflected shock wave propagates inside the pure gaseous phase from right to left, into state (1). The flow state obtained behind it is (4). The transmitted shock wave propagates inside the porous material, from left to right. The flow state behind it is (3). Since the porous material is flexible, its front edge, P, follows the transmitted shock wave. It should be emphasized here once again that the situation shown in figure 1(b), in which a transmitted shock wave exists inside the foam, is limited to short times following the head-on reflection and to regions in the vicinity of the front edge of the foam. This is due to the fact that the transmitted shock wave quickly decays to a dispersed wave, as shown in figure 1(c).

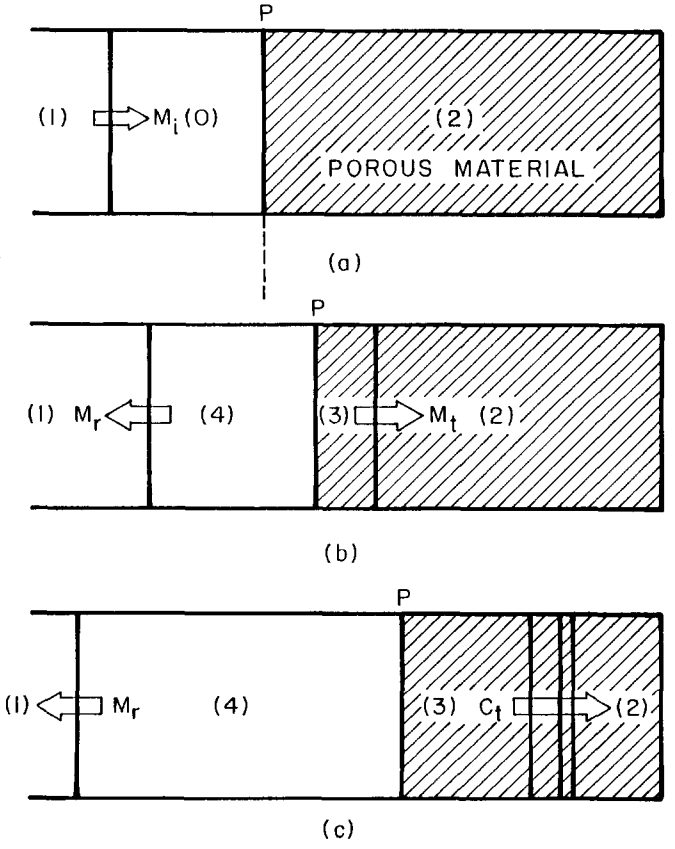

Figure 1. Schematic illustration of the wave pattern and definition of flow states (a) prior to the head-on reflection; (b) immediately after the head-on reflection; and (c) a long time after the head-on reflection.

The governing equations

The governing equations of the flow fields shown in figure 1(a) and (b) are as follows:

$$u_i = \frac{2a_j}{\gamma + 1}\left(M_k - \frac{1}{M_k}\right) \qquad [12a]-[14a]$$

$$p_i = p_j\left(\frac{2\gamma}{\gamma + 1}M_k^2 - \frac{\gamma - 1}{\gamma + 1}\right) \qquad [12b]-[14b]$$

$$a_i = a_j\frac{[2\gamma M_k^2 - (\gamma - 1)]^{1/2}[(\gamma - 1)M_k^2 + 2]^{1/2}}{(\gamma + 1)M_k} \qquad [12c]-[14c]$$

$$\rho_i = \rho_j\frac{(\gamma + 1)M_k^2}{(\gamma - 1)M_k^2 + 2} \qquad [12d]-[14d]$$

—across the incident shock wave: $i = 1$, $j = 0$ and $M_k = M_i$,
—across the transmitted shock wave: $i = 3$, $j = 2$, $u = \bar{u}$, $p = \bar{p}$, $a = \bar{a}$, $\rho = \bar{\rho}$ and $M_k = \bar{M}_t$.
—across the reflected shock wave: $i = 4$, $j = 1$ and $M_k = M_r$.
The matching conditions across the gas–foam interface P are:

$$\bar{p}_3 = p_4 \quad \text{and} \quad \bar{u}_3 = u_4 \qquad [15]$$

The above set of 14 governing equations is solvable provided the flow states (0) and (2) are given together with γ and M_i as initial conditions. The 14 unknown variables are u_1, p_1, a_1, ρ_1, $\bar{u}_3$, $\bar{p}_3$, $\bar{a}_3$, $\bar{\rho}_3$, u_4, p_4, a_4, ρ_4, M_r and $\bar{M}_t$.

The end-wall pressure

Skews' (1991) experimental results indicated that the shock wave transmitted into the porous material changes quickly to a dispersed compression wave. Based on this observation, the wave pattern shown in figure 1(b) transforms to that shown in figure 1(c). Consequently, the shock-tube end-wall is not hit by a shock wave but by a compression wave, which reflects back as a reflected compression wave. This is the reason for the failure of analytical models in which the pressure at the shock-tube end-wall was assumed to result from the head-on reflection of a transmitted shock wave. If one assumes that the flow region between the reflected compression wave and the

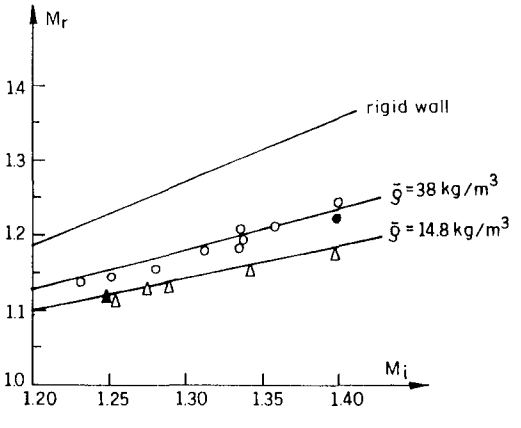

Figure 2. The dependence of the reflected shock wave Mach number, M_r, on the incident shock wave Mach number, M_i, for two different types of foam. The triangles correspond to the foam marked in table 1 as A and the circles to the foam marked as E. The open symbols are the experimental results of Skews (1991) and Skews *et al.* (1993) and the solid symbols are the numerical predictions of Olim *et al.* (1994). The solid lines are predictions of the presently proposed analytical model.

Table 1. Comparison between analytical and numerical predictions of the peak pressure at the shock-tube end-wall and the experimental results

Foam type†	M_i	$\bar{p}_{max}$ experimental‡	$\bar{p}_{max}$ analytical§	Relative error	$\bar{p}_{max}$ numerical¶	Relative error	$\bar{p}_{max}$ analytical‖	Relative error
A	1.27	378	390	3.1%	372	−1.6%	384	1.6%
B	1.29	421	504	17.9%	405	−3.9%	570	30.0%
C	1.40	910	1002	9.6%	—	—	1135	22.0%
D	1.27	420	497	16.8%	435	3.5%	565	29.4%
E	1.25	380	447	16.2%	—	—	506	28.4%
E	1.40	1071	1040	−2.9%	1025	−4.3%	1170	8.8%

†A, B and C are made of polyether with $\rho_p = 14.8$, 18.7 and 32.5 kg m/m^3; respectively. D and E are made of polyester with $\rho_p = 35$ and 38 kg m/m^3; ‡Skews (1991) and Skews *et al.* (1993); §present model; ¶Olim *et al.* (1994); ‖Gvozdeva *et al.* (1985). The pressures are in kPa.

Table 2. Comparison between analytical and numerical predictions of the front-edge velocity of the foam and the experimental results

Foam type†	M_i	u_f experimental‡	u_f analytical§	Relative error	u_f numerical¶	Relative error
C	1.40	58.2	65.4	11.6%	61.5	5.5%
E	1.40	54.5	61.4	11.9%	—	—

†Details of the foam-type are given in table 1; ‡Skews *et al.* (1993); §present model; ¶Olim *et al.* (1994). The velocities are in m/s.

shock-tube end-wall is a simple-wave-region, then the peak pressure at the shock-tube end-wall asymptotically reaches the stagnation pressure of the flow in state (3). Consequently, we propose

$$\frac{\bar{p}_{\max}}{\bar{p}_3} = \frac{\bar{p}_{t_3}}{\bar{p}_3} = \left[1 + \frac{\bar{\gamma} - 1}{2} \bar{M}_3\right]^{2\bar{\gamma}/\bar{\gamma} - 1} \quad [16]$$

where $\bar{p}_{t_3}$ is the stagnation (total) pressure of the flow in state (3).

COMPARISON WITH EXPERIMENTAL RESULTS AND DISCUSSIONS

Predictions of the above-described analytical model were compared to the experimental results of Skews (1991), Skews *et al.* (1993) and the numerical results of Olim *et al.* (1994).

A comparison between the analytical predictions of the reflected shock wave Mach number, M_r, and those measured experimentally for different incident shock wave Mach numbers, M_i, are shown in figure 2. Excellent agreement between the analytically predicted values and those measured experimentally or calculated numerically is evident for the lightest and heaviest foams. The reflected shock wave Mach number seems to almost linearly depend on the incident shock wave Mach number. The dependence of M_r and M_i for a head-on reflection from a rigid wall is also shown in figure 2. A comparison between various predictions of the maximum pressure developed at the shock-tube end-wall and the experimental results of Skews (1991) and Skews *et al.* (1993) is summarized in table 1. The various predictions consist of the analytical predictions of the proposed model [16], the numerical predictions of Olim *et al.* (1994) and the analytical predictions of the model proposed by Gvozdeva *et al.* (1985) in which incorrectly a transmitted shock wave was assumed to reach the shock-tube end-wall. It is evident from table 1 that the method for calculating the peak pressure at the shock-tube end-wall as proposed by the present analytical model is much better than that proposed by the analytical method of Gvozdeva *et al.* (1985) which was considered by Skews (1991) as a method having good predictions. The numerical predictions of Olim *et al.* (1994) which, in general, underestimate the experimental results, are superior to both analytical predictions. However, obtaining the analytical predictions is much easier and faster than obtaining numerical predictions.

A comparison between various predictions of the velocity of the front edge of the foam and the experimental results of Skews *et al.* (1993) is given in table 2. In view of the simplified model proposed in the present study, the predictions should be considered as quite good. Recall the fact that they were obtained without the need of conducting costly numerical simulations.

CONCLUSION

An analytical model describing the head-on interaction of planar shock waves with flexible porous materials was developed. Predictions of the analytical model were compared to experimental results and good agreement was evident.

A simplified method of calculating the peak pressure at the shock-tube end-wall was proposed. Predictions based on it were compared to experimental results and good agreement was obtained.

The good agreement between the experimental results regarding the peak pressure at the shock-tube end-wall and the analytical predictions of [16] provides a justification of the assumption that the end-wall pressure is actually equal to the stagnation pressure of the transmitted shock-wave induced flow field. In addition, since the predictions of [16] are based on the general analytical model which we developed the successful use of, [16] provides, in fact, a further validation of our model.

REFERENCES

Baer, M. R. 1992 A numerical study of shock wave reflections of low density foams. *Shock Waves* **2**, 121–124.

Gelfand, B. E., Gubanov, A. V. & Timofeev, E. I. 1983 Interaction between shock waves and porous screen. *Sov. Phys.-Fluid Mech.* **4**, 79–84.

Gvozdeva, L. G., Faresov, Yu. M. & Fokeev, V. P. 1985 Interaction between air shock waves and porous compressible materials. *Sov. Phys. Appl. Math. Tech. Phys.* **3,** 111–115.

Igra, O. & Ben-Dor, G. 1988 Dusty shock waves. *Appl. Mech. Rev.* **41,** 379–437.

Olim, M., van Dongen, M. E. H., Kitamura, K. & Takayama, K. 1994 On numerical simulation of propagation of shock waves in porous foams. *Int. J. Multiphase Flow* **20,** 557–568.

Rudinger, G. 1965 Some effect of finite particle volume on the dynamics of gas–particle mixture. *AIAA Jl* **3,** 1217–1222.

Skews, B. W. 1991 The reflected pressure field in the interaction of weak shock waves with compressible foam. *Shock Waves* **1,** 205–211.

Skews, B. W., Atkins, M. D. & Seitz, M. W. 1993 The impact of a shock wave on porous compressible foams. *J. Fluid Mech.* **253,** 245–265.